PNAS RESEARCH ARTICLE | EVOLUTION

Avian cranial kinesis is the result of increased encephalization during the origin of birds

Alec T. Wilken[a,1], Kaleb C. Sellers[a], Ian N. Cost[b], Julian Davis[c], Kevin M. Middleton[d], Lawrence M. Witmer[e], and Casey M. Holliday[f,1]

Affiliations are included on p. 10.

Edited by Zhonghe Zhou, Chinese Academy of Sciences, Beijing, China; received June 4, 2024; accepted January 13, 2025

The origin of birds represents a pivotal transition in vertebrate evolution, marked by significant changes in both brain size and feeding biomechanics. The evolution of the avian skull involved dramatic modifications, such as a segmented palate and the development of powered cranial kinesis in neognath birds. Powered kinesis, the ability to move parts of the skull independently, is considered a key innovation behind the dietary diversity and evolutionary success of birds. However, the processes driving the emergence of avian kinesis have remained unclear until recently. By analyzing data from Mesozoic birds, including reinterpretations of palate homology, 3D jaw muscle biomechanics, and linkage analysis, researchers have quantified changes in muscle forces and their effects on palate mechanics during the transition from theropods to birds. As the neurocranium expanded in non-avian theropods, temporal muscles shifted to more rostrocaudal positions in birds, aiding in the segmentation of the pterygoid. This musculoskeletal transformation increased fore-aft muscle force in neognaths, enabling powered cranial kinesis. A critical change was the separation of the epipterygoid ossification from the braincase, leading to the breakdown of primitive kinematic linkages and the development of a new basicranial joint, which allowed for greater cranial flexibility. These findings shed light on how the neurosensory and feeding systems coevolved during bird origins and offer new methods for identifying cranial kinesis in extinct vertebrates.

dinosaur | kinesis | biomechanics | skull | feeding

Significance

Biomechanical innovations are the underpinning of many great transitions in vertebrate evolution. The origin of birds is marked by radical transformations of the braincase, palate, and snout into a kinetic feeding system. New fossil discoveries hint that palate mechanics have played a crucial role in the diversification and success of birds, yet to date, there is no rigorous biomechanical framework for interpreting palate function in birds and other theropod dinosaurs. Here, we use three dimensional (3D) muscle modeling and linkage analysis to elucidate the origins of powered cranial kinesis in avian dinosaurs. Powered cranial kinesis did not evolve until neognaths. This study highlights the importance of integrating biomechanical modeling and phylogenetic methods for understanding key innovations in the origins of major clades.

Powered cranial kinesis in neornithine birds is a key innovation in vertebrate evolution, where, through a suite of changes, mobile linkages between the neurocranium and palate, driven by protractor muscles, enhanced craniofacial mobility (1–4). Powered cranial kinesis increases mechanical advantage of jaw muscles, improves craniofacial dexterity, and, consequently, expands dietary flexibility, all of which is thought to have enabled the subsequent evolutionary success and adaptive radiations of crown-clade birds (1–4). The origin of Aves was driven by an enlarging brain (5–7) associated with cognitive enhancements as well as the sensorimotor requirements of flight. Brain and thus skull shape changed drastically during avian evolution, likely causing changes in the palate and adductor chamber which houses the jaw musculature. However, the biomechanical relationship between increased encephalization, palatal morphology, and kinesis in birds remains untested, and thus, the evolution of the modern avian feeding apparatus remains poorly understood (3, 7, 8). Here, we show how using macroevolutionary biomechanics through 3D analysis of the musculoskeletal system, applied to living and extinct dinosaur and Mesozoic bird taxa, including *Ichthyornis* and *Hesperornis*, reveals the biomechanical cascade underlying powered avian kinesis.

Inferring cranial kinesis in extinct species has long vexed paleontologists (9, 10). Osborn (11) suggested kinesis based on the mobility of condylar joints in *Tyrannosaurus rex* but also noted that the linkages of surrounding bones would hinder movement. Indeed, many interpretations of kinetic capacity in extinct dinosaurs have relied on hypothesized mobility of presumed synovial joints and smooth, noninterdigitated sutures (e.g., refs. 12 and 13). However, these intracranial condylar joints and smooth, noninterdigitated sutures are likely features associated with growth and development, not necessarily mobility (8, 13, 14). Moreover, the debate over cranial kinesis has been hampered by confusing discussions focusing on either minute, vibrational movements that might occur passively during shock absorption, or the active, muscle-powered excursions of joints, which is the hallmark of avian-powered cranial kinesis. Diagnosing powered cranial kinesis in the ancestors of birds should rely on two main factors which govern mobility of intracranial joints: 1) the presence of forces acting on a joint to produce movement and 2) the linkage system of joints and bones that do not physically hinder movement (8, 14, 15). Here, we measured 3D jaw muscle resultants and scored the linkage systems of avian and non-avian theropod

Author contributions: A.T.W., K.C.S., I.N.C., J.D., K.M.M., L.M.W., and C.M.H. designed research; A.T.W., K.C.S., I.N.C., K.M.M., and C.M.H. performed research; A.T.W. and K.M.M. analyzed data; and A.T.W., K.C.S., K.M.M., L.M.W., and C.M.H. wrote the paper.

The authors declare no competing interest.

This article is a PNAS Direct Submission.

[1]To whom correspondence may be addressed. Email: atwilken@uchicago.edu or hollidayca@missouri.edu.

This article contains supporting information online at https://www.pnas.org/lookup/suppl/doi:10.1073/pnas.2411138122/-/DCSupplemental.

Published March 17, 2025.

dinosaurs to test for signals of powered cranial kinesis characteristic modern birds.

Protractor muscles (i.e., mm. levator pterygoideus and protractor pterygoideus) connect the neurocranium with the palate and play diverse roles in mediating kinetic excursions of cranial joints (14, 16). Electromyographic studies have demonstrated that protractor muscles are active during cranial kinesis in some neognaths (16); however, some akinetic species possess protractor muscles but do not display cranial kinesis (8, 17). Finite element modeling has shown that protractor muscles likely work to control unwanted kinetic movements and stabilize the palatobasal joint in lizards (13, 18) suggesting the avian condition of powered kinesis with permissive kinematic linkages is a derived one. Regardless, the diversity of protractor muscle functions can be attributed to many factors, such as muscle activation patterns, muscle architecture, and muscle orientation and position (14, 18). Muscle activation and architecture are impossible to study in fossils. However, comparing muscle force orientations has shown that the derived rostrocaudal orientation of protractor muscles in birds is necessary for fore-aft movements of the palate characteristic of avian-powered cranial kinesis (14).

Almost all dinosaurs possessed condylar, if not synovial palatobasal and otic joints (8, 13, 19). Recent studies have demonstrated, however, that joint tissue composition is not necessarily indicative of mobility. For example, Wilken et al. (18) illustrated through finite element modeling that changing intracranial joint tissues does not significantly affect loading at these joints. Moreover, Mezzasalma et al. (15) found that gross morphology of cranial joints better explains kinetic capacity in lizards than does histology. Furthermore, birds with bichondral otic joints are just as capable of streptostylic rotation of the quadrate as are lizards with unichondral otic joints (20–23).

The evolution of the bird skull is characterized by an elimination of bony elements that ultimately resulted in kinetically permissive linkages (4, 8). The avian kinetic linkage system is a parallel four-bar linkage wherein the quadrate pushes the strut-shaped palate and jugal bar rostrally, elevating the beak (14, 24, 25). The overall mobility of this four-bar linkage can be quantified by degrees of freedom (4). The upper temporal bar (composed of squamosal and postorbital bones) and the postorbital bar (jugal and postorbital) prohibit kinetic excursions (7, 23, 25–28). Reduction of these bony connections was then key to establishing avian-style cranial kinesis (2, 8, 28–34). Cranial forces, such as moments generated about cranial joints by muscle and bite forces, oriented in other potentially disadvantageous directions would make the feeding apparatus perform suboptimally and potentially fail. Like the bones of the face (e.g., premaxillae, maxillae, nasals), the tall, thin, braced palatal bones (e.g., palatine, pterygoid, epipterygoid) of most non-avian dinosaurs were also primarily oriented to resist dorsoventral forces (14). Because kinetic linkages often require strut-like or tubular morphologies that can resist a diverse array of axial loading, torsional loading, and bending environments created by different kinetic feeding postures (13, 14, 18), we expect concomitant changes to evolve in the muscles powering the system. Thus, the acquisition of strut-like, propulsive pterygoid, palatal, and cheek elements along the line to birds not only reflects a drastic shift in loading patterns of the facial elements but also of the palate, the jaw muscles, and the protractor muscles, all of which contribute to the origin of cranial kinesis.

Most of the features associated with cranial kinesis can be explained by changes in muscle force direction, and it has been noted by many authors that birds have a markedly rostrocaudal orientation of jaw muscles [Fig. 1; (8, 14, 26, 35, 36)]. What then is the cause of the alteration of muscle force vectors in the theropod cranium? Brain size is a driving force of theropod dinosaur cranial anatomy [Fig. 1; (5, 7, 36, 37)]. Moreover, extreme expansion of the brain in birds did not occur until Neoaves (37), apparently coinciding with the evolution of kinetically permissive linkages, intracranial joints with a morphology suggestive of mobility, and rostrocaudally oriented protractor muscles (8, 14, 35). Although it has been recognized that lateral expansion of the braincase profoundly alters the adductor chamber [Fig. 1; (8, 35, 36)], how lateral expansion of the braincase changes position and force production of jaw muscles as well as cranial mechanics remains unknown. Here, we show that lateral expansion of the braincase resulting from phylogenetic brain size increase, shifted temporal muscles into rostrocaudal orientations, decreasing orthal feeding efficiency while instead decreasing mediolaterally oriented protractor muscle forces and shifting to propulsive efficiency in the palate. All the while, drastic changes in palatal morphology in Ornithurans set the stage for increased mobility (Fig. 2). These biomechanical changes following brain expansion, along with trends in miniaturization and the decoupling of the epipterygoid to the braincase, were likely responsible for enabling more permissive kinematic linkages to evolve in neoavians.

When powered cranial kinesis evolved within birds also remains unclear. Whereas early diverging avian lineages like jeholornithids, confuciusornithids, and enantiornithines appear to have maintained a relatively primitive shape and number of cranial linkages and bones (27–33), Ornithurans such as *Ichthyornis* significantly eliminated cranial linkages and evolved potentially flexible palates (3, 7). Here, we explore this hypothesis using 3D muscle reconstruction, 3D lever analysis, linkage analysis, and comparative methods using a sample of non-avian theropods, ichthyornithes, hesperornithes, paleognathe, and neognathe birds.

Results

We found a cascade of changes occurred in the cranial morphology of theropod dinosaurs that is likely the result of an expanded neurocranium. The concatenate change in temporal fossa position changed the orientation of jaw muscles toward a more rostrocaudal orientation. This positional shift in musculature reoriented muscle loading vectors about the linkage system of the palate and suspensorium causing joints to release loads through kinetic excursions while also changing the shape of the palate from the primitive braced frame to a propulsive shape (14). Three dimensional models can be found in (https://osf.io/2kpdb/) (38).

Jaw muscles are more rostrocaudally oriented in birds compared to the dorsoventrally oriented jaw muscles of non-avian dinosaurs (Fig. 1 *B*, *D*, and *E*). Temporal muscles like mAMEP show a gradual transition from dorsoventral orientations in non-avian dinosaurs, while mAMES shows a bimodal distribution of extremely dorsoventral orientations in non-avian dinosaurs and rostrocaudal orientations in birds (Fig. 1 *D* and i). Conversely, orientations of mPtd are largely rostrocaudal in non-avian dinosaurs and shift to dorsoventral orientations in birds (Fig. 1 *D* and *E*). Birds rely on more equal distribution of jaw muscle forces compared to the more pterygoideus-dominant system non-avian dinosaurs (*SI Appendix*, Fig. S1).

We found appreciable changes in the sizes of jaw muscles relative to the expansion of the braincase (Fig. 1*A*). Qualitatively, there is a noticeable negative trend between braincase expansion and size-corrected jaw muscle volume (Fig. 1*A*). This trend is best illustrated by exemplar taxa, such as *Dromaeosaurus* and *Corvus*. *Dromaeosaurus* has a relatively narrow braincase (braincase width/biquadrate width = 0.34), but a robust amount of jaw muscle volume relative to its head size (jaw muscle volume residual = 1.8).

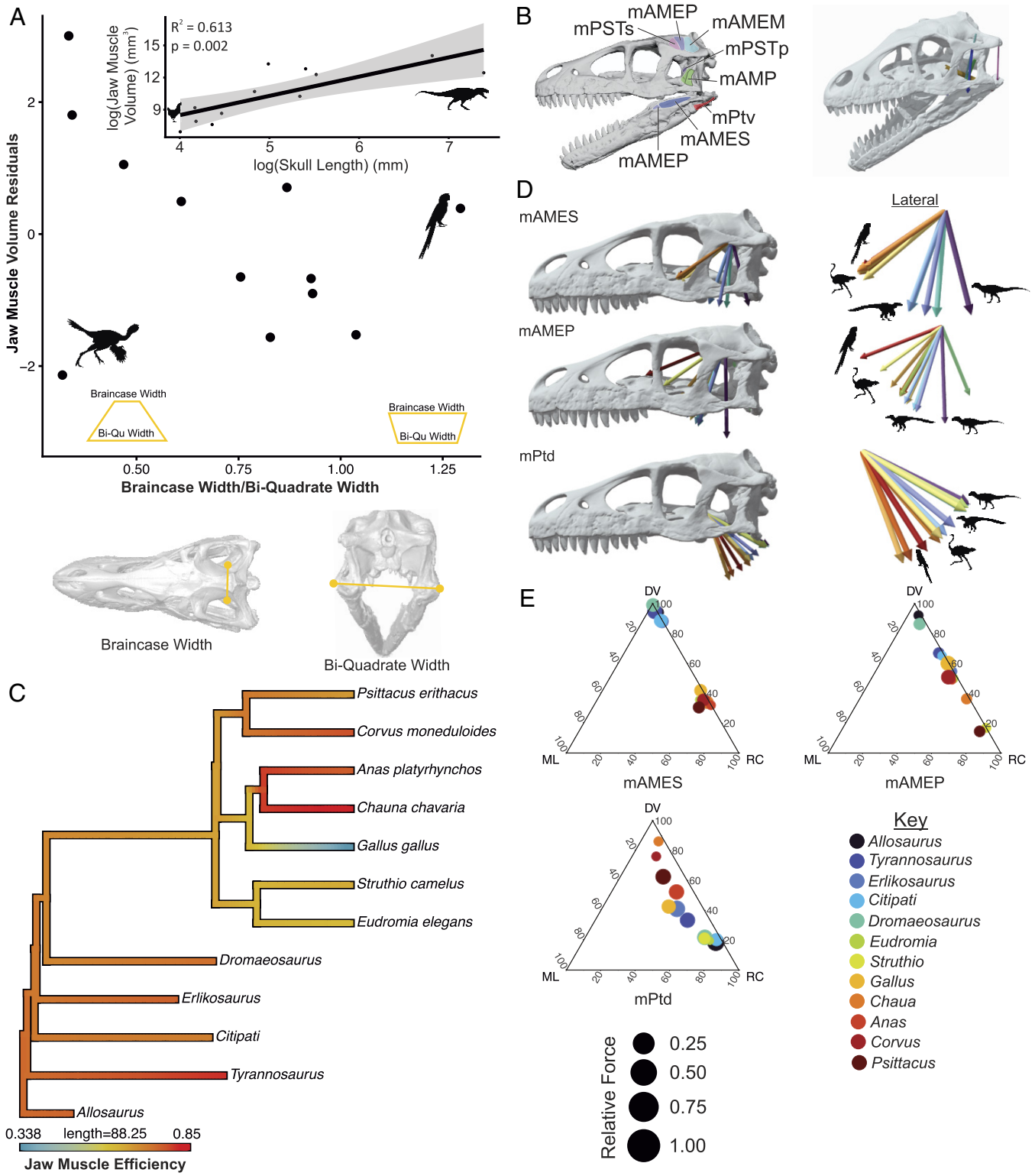

Fig. 1. Increased encephalization changed orientations of jaw muscles during avian evolution which led to a decrease in orthal efficiency of the muscles. (*A*) the relationship between relative braincase width and total jaw muscle volume shows the neurocranium became wider dorsally during avian evolution while jaw muscle volume did not appreciably change. (*B*) Jaw muscle attachment sites and 3D vectors of jaw muscles in non-avian theropods as shown by *Dromaeosaurus*. (*C*) Phylogenetic trends in jaw muscle vectors show avian jaw muscles became less efficiently oriented as they shifted from orthal (vertical) orientations to rostrocaudally diagonal orientations. (*D*) Evolutionary changes in the 3D resultant vectors of jaw muscles show a shift from vertically oriented, to diagonally oriented temporal muscles and shift from transversely oriented to parasagittally oriented protractor muscles. Taxon-specific muscle vectors are superimposed on *Dromaeosaurus* (AMNH 5356) to illustrate these patterns. (*E*) 3D jaw muscle orientations of non-avian theropods and extant birds changed markedly where many temporal muscles shifted from near vertical to more rostrocaudally sloped orientations, pterygoideus muscles shifted to more rostrocaudally sloped orientations, and protractor muscles also shifted from transverse orientations to rostrocaudally sloped orientations. All of these shifts together reflect a change from orthally oriented cranial loads during feeding to fore-aft loads during feeding. DV, dorsoventral; ML, mediolateral; RC, rostrocaudal; mAMEM, m. adductor mandibulae externus medialis; mAMEP, m. adductor mandibulae externus profundus; mAMES, m. adductor mandibulae externus superficialis; mAMP, m. adductor mandibulae posterior; mPSTp, m. pseudotemporalis profundus; mPSTs, m. pseudotemporalis superficialis; mPtd, m. pterygoideus dorsalis; mPtv, m. pterygoideus ventralis.

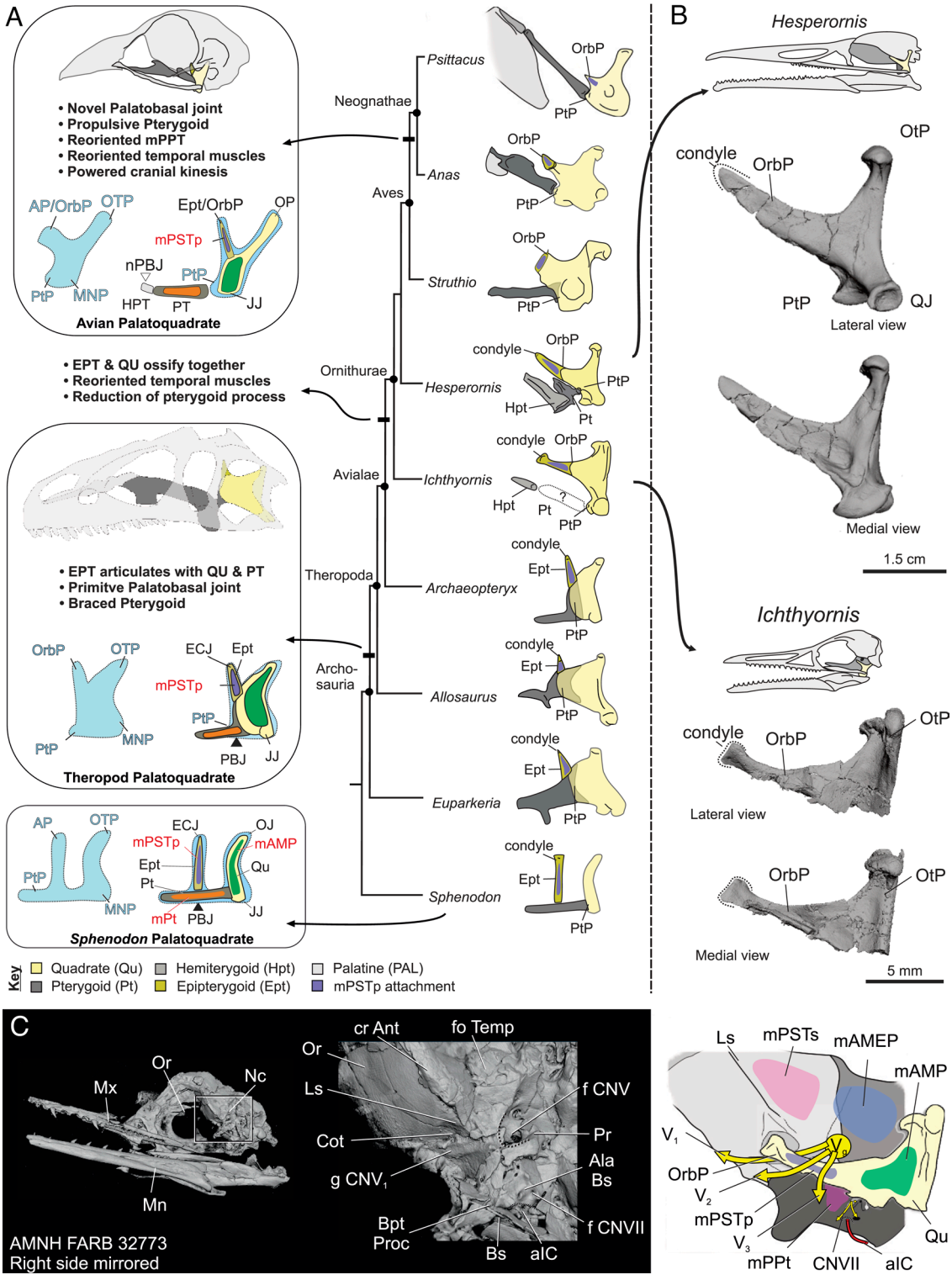

Fig. 2. Evolutionary and developmental transformational hypotheses of the palate and palatoquadrate cartilages during avian evolution reveal powered cranial kinesis did not evolve until Neognathae. (*A*) Stepwise changes in palatal morphology along the line to modern birds reveal changes in 3D muscle resultants and linkage breakdowns necessary for powered cranial kinesis were not present until Neognathae. Changes in adult morphologies are best explained by a developmental transformation in the palatoquadrate cartilage and the synonymy of the ascending process, epipterygoid, and orbital process of the quadrate. (*B*) New imaging data of *Hesperornis* and *Ichthyornis* reveal a breakdown in the articulation of the palatoquadrate cartilage and neurocranium. (*C*) Interpretation and reconstruction of soft tissues in the temporal fossa of *Ichthyornis* (AMNH FARB 32773) reveal the orbital process of the quadrate articulates with the laterosphenoid akin to the epipterygoid-laterosphenoid joint of non-avian dinosaurs, limiting kinetic capacity. Abbreviations: aIC, Internal carotid artery; ala Bs, ala basisphenoid; AP, Ascending process of PQ cartilage; CNVII, facial nerve; Cot, cotyle for OrbP; Cr Ant, antotic crest; ECJ, Epipterygoid-cranial joint; Ect, Ectopterygoid; Ept, Epipterygoid; f aIC, foramen for internal carotid artery; F CNV, foramen for trigeminal nerve; f CNVII, foramen for facial nerve; fo Temp, temporal fossa; g CNV1, groove for ophthalmic nerve; HPt, Hemipterygoid; JJ, Jaw joint; Ls, laterosphenoid; MnP, Mandibular process of PQ cartilage; mAMEP, m. adductor mandibulae externus profundus; mAMP, m. adductor mandibulae posterior; mPTSp, m. pseudotemporalis profundus; mPSTs, m. pseudotemporalis superficialis; mPT, m. pterygoideus; Mn, mandible; Mx, maxilla, Nc, neurocranium; nPBJ, novel palatobasal joint between HPt and parasphenoid rostrum; PQ, palatoquadrate cartilage; Or, orbit; OrbP, Orbital process of PQ cartilage; OrbP, Orbital process of quadrate; OtP, Otic process of quadrate; OtJ, Otic joint; Pa, palatine; PBJ, Palatobasal joint between pterygoid and basiphenoid; Pt, pterygoid; PtP, pterygoid process of quadrate; Pr, prootic; proc Bpt, basipterygoid process; Qu, Quadrate; V1, ophthalmic nerve; V2, maxillary nerve; V3, mandibular nerve; Vg, trigeminal ganglion.

Conversely, *Corvus* has a relatively wide braincase (braincase width/biquadrate width = 0.79), but a small amount of jaw muscle volume relative to its head size (jaw muscle volume residual = −1.53). Despite being the largest of its kind to date, our sample size is too small to perform meaningful statistical analyses to find a quantitative relationship. Given the disparate cranial morphologies, feeding adaptations, and independent phylogenetic evolutions of our taxa sampled, ranging from oviraptors to tyrannosaurs to chickens, even these preliminary, qualitative insights suggest a relationship between brain size, skull width, and muscle volume that merits further investigation.

Mapping jaw muscle efficiency on a phylogeny of theropods reveals stepwise patterns in feeding mechanics and generates hypotheses of jaw muscle function in Mesozoic birds, for which there is a dearth of 3D data (Fig. 1*C*). All the non-avian theropods sampled here have relatively high jaw muscle efficiency for orthal biting, reflecting relatively vertical muscles. In contrast, birds demonstrate more diversity in jaw muscle efficiency, reflecting the higher diversity of jaw muscle arrangements away from pure vertical, as illustrated by the muscle vectors in ternary space (Fig. 1 *C–E*). Remarkably, the long branch to modern birds teases a decrease in jaw muscle efficiency in Mesozoic birds that will require additional investigation. We hypothesize the similarity in jaw muscle efficiency between some of the modern birds, like parrots, and non-avian dinosaurs like *Citipati* is convergence in harder-biting performance that was likely re-evolved during the radiation of modern birds of the Tertiary (39).

We employed linkage analysis to evaluate the interactions among the many cranial joints in the theropod head and use this evidence to estimate an origin for a mobile cranium in the theropod lineage. To do this, we first conducted a survey of cranial joint and palate morphologies across theropods (Fig. 2) and scored the degrees of freedom of each individual joint in the cranium based on descriptions from the original publications. These scores can be found in Dataset S1. Although condylar palatobasal joints and otic joints are ancestral to theropods and archosaurs broadly (8), the highly overlapping scarf joints, ubiquitous throughout the rest of the cranium is observed until crown Aves. These immobile scarf joints restrict mobility elsewhere in the cranium (Fig. 3), creating a linkage system best illustrated here by *Allosaurus* (Fig. 3*D*). In this early-diverging theropod cranial linkage system, the net degrees of freedom (DoF) is calculated to be -10. We interpret this to mean this cranial morphotype is not a mobile linkage system and is therefore akinetic.

This cast of morphological features, including a braced palate, epipterygoid articulating with the laterosphenoid, and sutured dermatocranial elements is found in *Allosaurus*, earlier diverging coelurosaurs as well as *Archaeopteryx* and enantiornithines (although to date there is no reported epipterygoid for an enantiornithine), suggesting akinesis was a feature of the clade until Neognathae (Figs. 2 and 3). Although *Ichthyornis* and *Janavis* have been hypothesized to have a tubular pterygoid akin to neognathes (3), here, we agree with Dyke et al. (40) that the alleged pterygoid bone of *Janavis* is in fact a coracoid. The element possesses a clear, flared sternal process and partial glenoid fossa which would articulate with the humerus (see *SI Appendix*, Fig. S14 for further discussion of this point). Therefore, we still lack a pterygoid for Ichthyornithes. Meanwhile, we do identify a cotyle for the articulation of the epipterygoid or orbital process of the quadrate on the right side of AMNH FARB 32773. As in other archosaurs and dinosaurs, the epipterygoid cotyle resides just dorsal to the groove for the ophthalmic division of the trigeminal nerve and ventral to the antotic crest, which separates the temporal fossa from the orbit [Fig. 2*C*; (34)]. Other neighboring identifiable structures supporting this interpretation include the fractured trigeminal fossa and foramen, the facial nerve exiting the braincase next to a fractured ala basisphenoid and internal carotid foramen. When the quadrate is articulated with the still-present otic cotyle of the squamosal-prootic, the mitten-shaped condyle of the quadrate orbital process fits in the cotyle suggesting the quadrate and pterygoids remained fully articulated with the neurocranium in *Ichthyornis*. Thus, reevaluation of Ichthyornithes and *Janavis* suggests that their cranial material still lacks evidence of a neognath-like pterygoid, supporting the presence of a primitive palatobasal joint and palatoquadrate-laterosphenoid joint as in other *Archaeopteryx* and likely other Mesozoic birds. Despite these changes in the palatal elements of Mesozoic birds, the palatobasal joint remains primitive until Neognathae, where a condylar growth plate persists between the pterygoid bone and the basisphenoid. With the ejection of the coracoid from the head of Ichthyornithes, we must dispel the hypothesis that the neognathan HPT-PRJ (a.k.a. "novel PBJ") was present in these Mesozoic birds. Therefore, we do not find evidence of a propulsive pterygoid or a permissive linkage morphology necessary for powered cranial kinesis in Ichthyornithes (Figs. 2 and 3).

The first definitive departure from the primitive braced pterygoid appears to be in *Hesperornis*, which has a small, peculiar pterygoid with a quadrate articulation that has both a triangular, braced component, as well as novel condylar articulation(Figs. 2 *A* and *B* and 4). *Hesperornis* has also been interpreted to have a long, mediolaterally flat, braced hemipterygoid bone that articulates with the palatine. Understanding how these elements articulate is flustering. The most current reconstruction of the palate of *Hesperornis* (41), where the small concave quadrate process of the putative pterygoid articulates with a noticeable convex articular surface on the body of the quadrate between the orbital process and articular condyles, would have the large muscular process of the pterygoid extending ventrally, likely intersecting through the mandible when articulated, if not at best, bracing the mandible from wishboning. Additionally, the putative hemipterygoid in *Hesperornis* [Fig. 2*A*; (41, 42)] appears to articulate with the lateral surface of the pterygoid, rather than the rostromedial surface of the element as found in other birds, and, as with the descending flange of the pterygoid, would interfere with the mandible. This said, without other evidence, we are currently unable to propose an alternative reconstruction of the palate and defer to Gingerich (41). Regardless, the orbital process of the quadrate of *Hesperornis* is long, thin, and tapering, departing from the condylar shape of the process in Ichthyornis. Although a small condyle-like articular surface is visible on the orbital process of the quadrate, no complementary cotyle can be found on the braincases of *Hesperornis*, albeit, they are all crushed dorsoventrally. This suggests the quadrate may be able to pivot more independently from the neurocranium in *Hesperornis* than in more earlier diverging lineages.

The palatal morphologies of *Ichthyornis* and *Hesperornis* suggest earliest experiments in cranial kinesis may be found at the base of Ornithurae. We find net mobility in *Ichthyornis* (Fig. 3*C*). Despite the lack of a pterygoid for Ichthyornithes, the surrounding articulations with the quadrate and palatine tease a mobile caudal palate (Fig. 3*C*). This mobility is restricted to the caudal palate, however. Streptostylic excursions of the quadrate may have been possible, resulting in a DoF of 4. In *Hesperornis*, the unique, triangular pterygoid and long, overlapping hemipterygoid (42) present no evidence for a mobile palate, resulting in a DoF of 0. Other permissive linkages, such as the craniofacial hinges, or inferences of streptognathy or rhynchokinesis require more testing (43, 44). Clear craniofacial hinge joints are not present until Neoaves. The hypothesized flexibility of the long, frontonasal scarf joints in

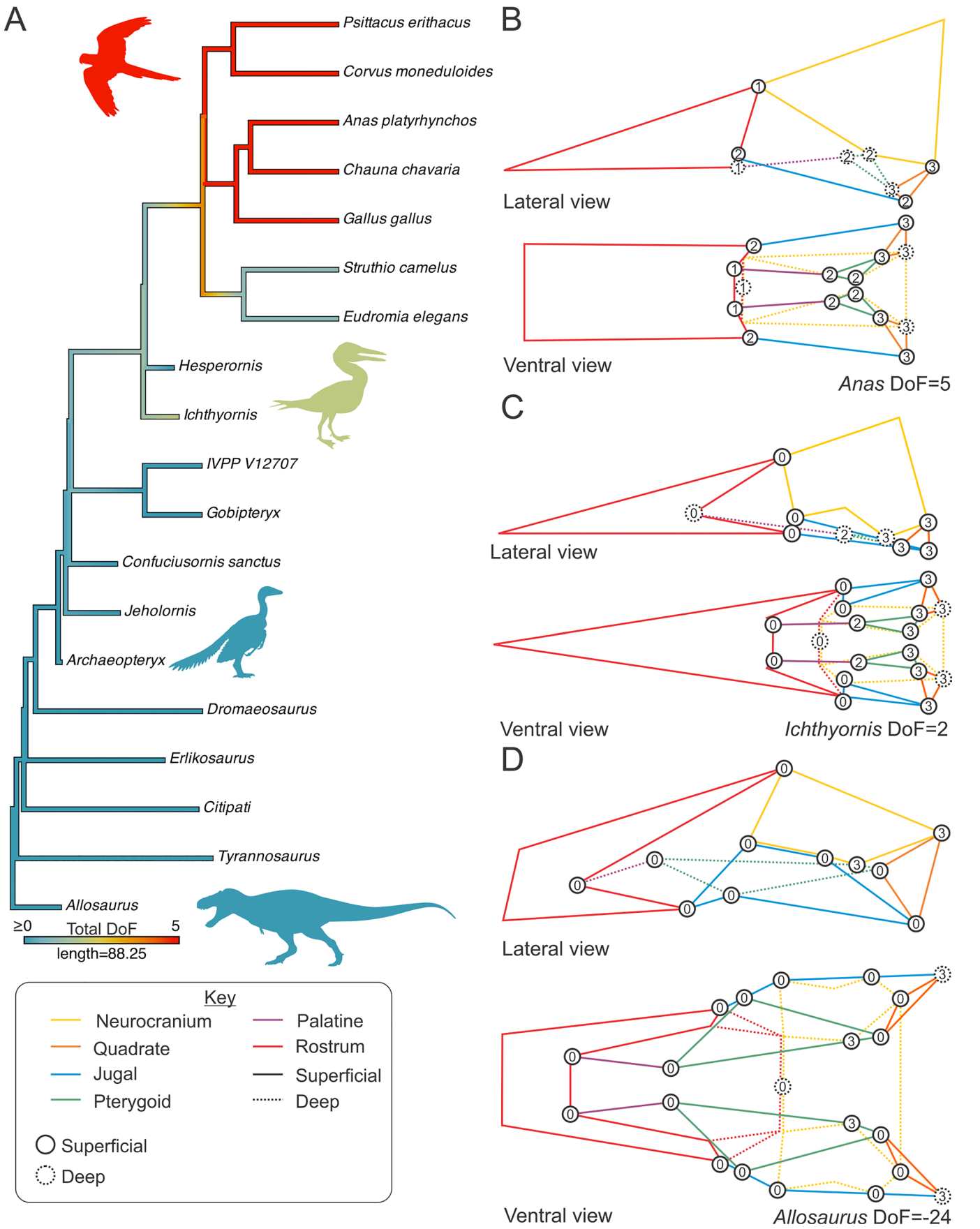

Fig. 3. Cranial linkages broke down in a stepwise fashion during avian evolution following the increased encephalization and reorientation of temporal muscles, resulting in powered cranial kinesis within Neognathae. (*A*) Phylogenetic patterns in cranial linkages across during the origin of birds. (*B*) Cranial linkage system of *Anas,* (*C*) Cranial linkage system of *Ichthyornis.* (*D*) Cranial linkage system of *Allosaurus.* Linkages are scored based on articulations at each joint (integer in circle) and loops of elements (colored in Key).

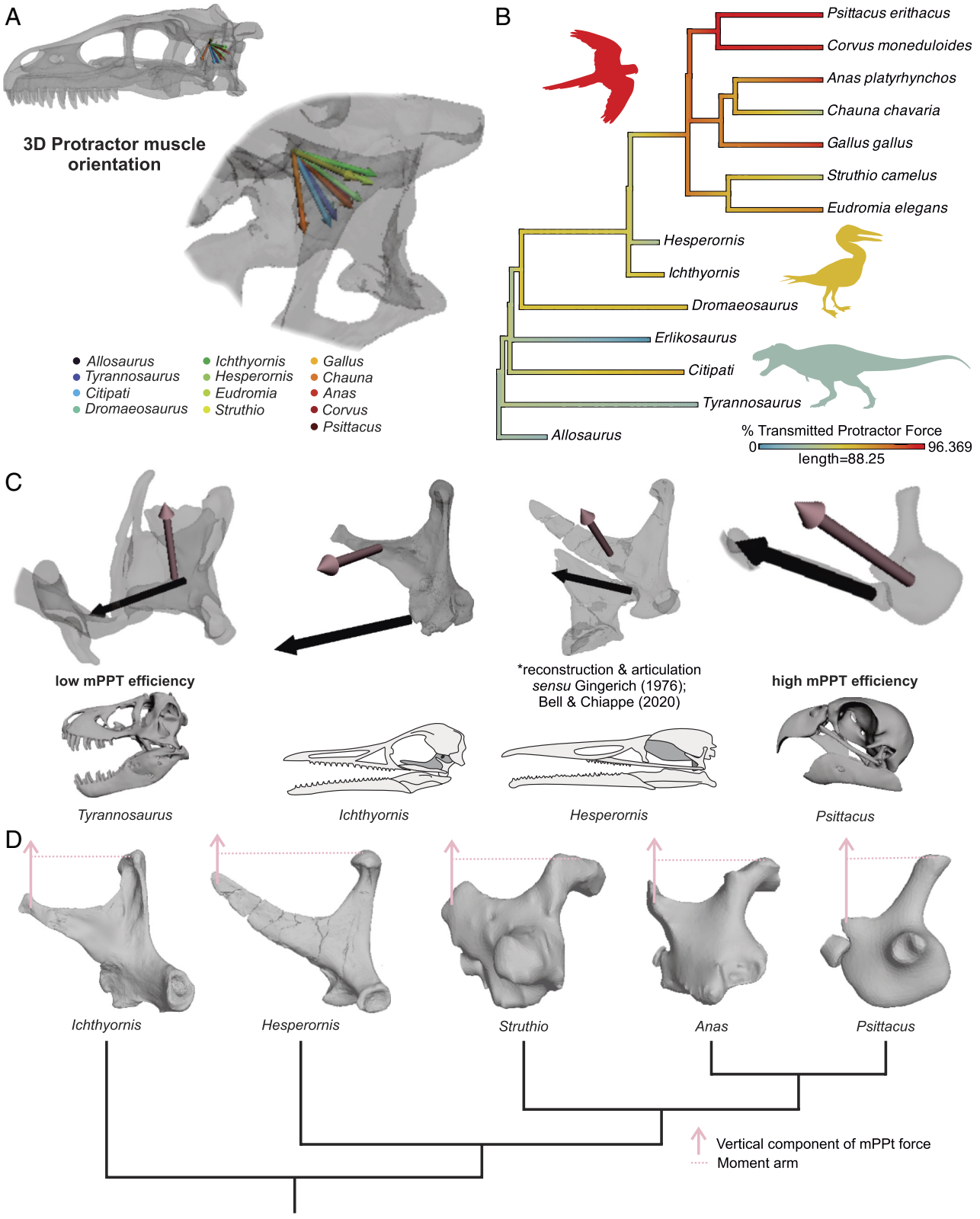

Fig. 4. Protractor muscle forces changed in orientation and relative loading during the theropod-bird transition, ultimately promoting powered cranial kinesis in birds. (*A*) Variation in 3D protractor muscle orientations in the sample projected from a shared origin on the skull of *Dromaeosaurus* with each colored vector being from a different taxon. (*B*) Transmitted protractor muscle force changed from transverse, postural orientations (blue-gray) to fore-aft orientations (red) along the line to birds, resulting in powered cranial kinesis in anseriforms and Neoaves. projected onto the skull of *Dromaeosaurus*. (*C*) Reorientation of protractor muscles coevolved with the shape of the pterygoid along the line to birds. *Tyrannosaurus* and other nonornithurine theropods possess braced pterygoids and transversely oriented protractor muscles that work orthogonal to the orientation of the pterygoid. Although *Ichthyornis* (AMNH FARB 32773) possesses a segmented, potentially propulsive pterygoid, the protractor muscles have yet to reorient to the efficient, fore-aft orientations found in birds with powered cranial kinesis such as *Psittacus*. (*D*) The long, rostrally projecting orbital process of the quadrate in the stem birds *Ichthyornis* and *Hesperornis* increases the moment arm of m. protractor pterygoideus about the otic joint.

Hesperornis and other Mesozoic birds needs to be tested more to determine whether this was enough deformation to escape the largely immobile cranium we find here. Without a mobile palate, biologically meaningful excursions at the craniofacial hinge are limited, regardless of the potential mobility of the craniofacial hinge in isolation (Fig. 3).

Finally, the cranium of Neognathe exhibits net mobility, as shown by *Anas* (Fig. 3*B*). The largely mobile joints within the palate and facial skeleton allow for total DoF of 5. The increased mobility found throughout the cranium allows for excursions at the craniofacial hinge and thus fully accomplished prokinesis.

Regardless, the constellation of an enlarged orbital process, condylar otic joint and diminishing contacts between the quadrate, pterygoid, palatine, and quadratojugal suggests the possibility for limited streptostyly at the base of Ornithurae (Fig. 3*A*). The akinetic palate of *Hesperornis,* suggests the hopeful cranial kinesis of *Ichthyornis* may be derived compared to other taxa in its broader phylogenetic grade (Fig. 3*A*). Our ancestral state reconstruction suggests a partially kinetically competent cranium was present near the origin of crown Aves (Fig. 3*A*) but also living paleognathes may have secondarily lost this competency. Therefore, we find fully mobile crania were not acquired until Neognathae (Fig. 3*A*).

Changes in palatal morphology coincided with shifts in protractor muscle function likely then impacting propensity for powered kinesis (Fig. 4). Whereas protractors largely served as mediolaterally oriented postural muscles bracing the palate in non-ornithuran dinosaurs, once the orbital process was freed from the braincase articulation, they shifted into more rostrocaudally oriented vectors more capable of modulating streptostylic movements of the quadrate and pterygoid. A less understood prerequisite for a propulsive pterygoid is how much protractor muscle force is transmitted axially through the pterygoid (Fig. 4). Lower transmission of protractor muscle force implies that protractor muscle force vectors are more orthogonal to the pterygoid (e.g., Fig. 4 *B* and *C*: *Tyrannosaurus*; *Ichthyornis; Hesperornis*) pulling the palate mediolaterally toward the neurocranium, counteracting the consistently lateral pull by the pterygoideus muscles. Novel, more rostrally oriented protractor muscles enable more efficient propulsive force transmission in tinamous, ducks, and neoavians and tracks with the increasingly fore-aft, craniocervical behaviors characteristic of birds (Fig. 4 *A* and *B*). Our sample shows that only neognaths possess both tubular pterygoids and propulsively oriented protractor muscles suggesting powered cranial kinesis is likely only a neognath feature. *Ichthyornis* and *Hesperornis* did not possess the muscles capable of powering the fore-aft movement necessary for the behavior (Fig. 4 *B* and *C*).

Discussion

Avian-powered cranial kinesis evolved as a biomechanical cascade, lagging behind the increased encephalization seen along the line to birds, but was not possible until a series of musculoskeletal innovations occurred. Braincase expansion shifted jaw muscle vectors, leading to a breakdown of linkages, reorientation of protractor muscles, and ultimately a propulsive palatal behavior. The change in orientation of jaw muscles following encephalization and neurocranial shape change is one of the key drivers of avian skull function and feeding behavior. The positional shift of temporal muscles, from primitively vertical to rostrocaudally diagonal orientations likely unloaded the jaws and face from orthal forces. As the efficiency of vertical muscles and orthal biting waned, the avian feeding apparatus evolved into a new envelope of musculoskeletal function and behavioral diversity where, alongside inertial feeding (45), fore-aft shear forces became more prevalent. We hypothesize that this change in loading regime (orthal to shear) was likely responsible for evolution of strongly recurved teeth in dromaeosaurs, followed by the eventual replacement of teeth for multidirectionally mechanically resistant keratinous beaks in birds (46).

While the skulls of non-avian theropods possessed several condylar intracranial joints, these skulls still possess high linkage scores via temporal bars and palatal elements as well as mediolaterally oriented protractor muscles that stabilized and stiffened the skull (13, 14). The freed quadrate orbital process and reoriented protractor muscles were paramount musculoskeletal transformations that were necessary to achieve powered kinesis prior to the acquisition of a clear craniofacial hinge. Other forms of kinesis, such as rhynchokinesis, might appear in paleognath birds (44), but the cranial morphology of these animals is adapted to resist any significant kinetic excursions (19). Powered prokinesis likely only evolved in Neognathae (Fig. 4).

Although our sampled neognath birds demonstrate a diversity of jaw muscle arrangements, reflecting the spectacular trophic diversity of the modern clade, we suspect a similar 3D analysis of the skulls of Mesozoic species will reveal a bottleneck of musculoskeletal morphology near the origin of crown birds where the breakdown of temporal bars and temporal muscle reorganization co-occur. Like in confuciusornithids, various extant bird lineages evolved solutions to these inefficient jaw muscle orientations by developing secondary temporal arcades formed by mineralized aponeuroses (28, 47). These novel bony bars enable the temporal muscles to reoccupy more vertical, orthal orientations and expand the surface area of bony attachment. While temporal muscle loading changed, pterygoideus musculature orientations and forces remained rather consistent. So, whereas the fore-aft loading orientations of m. pterygoideus were in part counteracted by orthal loads of temporal muscles in non-avian theropods, the reoriented temporal muscles of birds instead act synergistically to create fore-aft loads and ultimately promote powered avian kinesis.

Despite the earlier acquisition of flight and small body size, Mesozoic birds including *Archaeopteryx*, jeholornithids, confuciusornithids, and enantiornithines retained similar temporal and palatal morphologies of dromaeosaurs and other non-avian theropods including braced pterygoids, ectopterygoids, epipterygoids, condylar palatobasal joints, and presumably orthally oriented temporal muscles [(28–33, 48), Fig. 1]. Even Ichthyornis appears to still possess condylar palatobasal joints and additional articulations between the quadrate and braincase. Meanwhile, there is currently a gulf of missing information linking the palatal morphologies found in ornithurine birds from those found in earlier diverging clades. In particular, we are missing species that possess transitional morphologies revealing how the pterygoid shifted from a tall, thin, braced morphology still found in *Hesperornis*, to the intermediate shape found in paleognathes, to the tubular shape found in neognathes. Additionally, we lack transitional forms that reveal how the quadrate evolved the orbital process. When the fossil record fails to provide clear phenotypic transformations, we can look to patterns in developmental biology.

We propose the orbital process of the quadrate in *Ichthyornis, Hesperornis,* and other birds is actually the epipterygoid, explaining the so-called loss of the element. The orbital processes of *Ichthyornis* (AMNH FARB 32773) and *Hesperornis* (KUVP 71012) are incredibly long (Figs. 2*B* and 4*D*) and possess articular condyles that still likely articulated with the laterosphenoid (Fig. 2*C*). The epipterygoid and quadrate are both endochondrally ossified portions of the palatoquadrate cartilage and it is reasonable to predict the two elements can maintain close association through development and evolution (Fig. 2). Previous studies of avian cranial development

illustrate the orbital process [sensu Crompton (47); sensu ascending process of de Beer (49); sensu "pterygoid process" of other avian developmental biologists (50)] of the palatoquadrate emerges from the cartilaginous body of the quadrate while the pterygoid bone membranously ossifies from a separate population of mesenchyme (51). This differs from the putative primitive reptile condition in *Sphenodon* where the ascending process (sensu orbital process) of the palatoquadrate is separated from the quadrate condensation by the ossification of the pterygoid. We envision that the palatoquadrate cartilage of primitive archosaurs does not look like the palatoquadrate cartilage of *Sphenodon* and lepidosaurs, but instead is a large, shield-shaped cartilage, which has clear otic, mandibular, and orbital (ascending) process emerging from the body of the cartilage, where the pterygoid process is merely the rostroventral corner of the cartilage [Fig. 2; (47, 49–52)]. The presence of both the putative orbital process and the mineralizing pterygoid bone near the pterygoid process demonstrate the two structures are not homologous via the test of conjunction. Topologically, the lateral surface of the bony orbital process of the quadrate remains an attachment site for mPSTp, similar to the epipterygoid of non-avian dinosaurs and all other diapsids [Fig. 2; (34)]. Similarly, both the orbital process of the quadrate and the epipterygoid form a bony divide between the ophthalmic nerve (V_1) and the maxillary nerve [V_2; Fig. 2; (34)]. This cast of characters demonstrates the epipterygoid and its attachments remained fixed to the quadrate during avian development and evolution. At minimum, the presence of a pronounced orbital process of the quadrate shows Ornithurae grade stem birds possess adductor chamber anatomical topology reminiscent of crown Aves. A refined fossil record of the quadrate, epipterygoid, and palate in stem birds such as jeholornithids, confuciusornithids, and enantiornithines will be needed to test this hypothesis.

Given the fossil record, we remain challenged to confidently diagnose powered cranial kinesis in birds outside Neoaves. We find *Ichthyornis* might be an early evolutionary experiment in cranial mobility, having 4 degrees of freedom, but insignificant protractor muscle force transmission through the palate (Figs. 3 and 4). Hopeful kinesis can be viewed as an unstable palate, creating a novel motor control problem for feeding in monsters like *Ichthyornis* and *Hesperornis* (e.g., refs. 18 and 53) where these birds may have to had coordinate potentially pathological pushing and pulling of the posterior palate using *m. protractor pterygoideus*. Because the frontonasal joint does not show evidence of mobility in *Ichthyornis* or *Hesperornis,* the adaptive benefits of cranial kinesis in extant birds, such as having a dexterous upper beak (e.g., ref. 35) or increasing mechanical advantage for jaw musculature (1, 25), are not viable for these stem birds. We are currently unable to quantitatively test for intrabone flexibility (e.g., streptognathy, rhynchokinesis) which has been proposed for these animals in the past (43, 44). The protractor muscle force of *Ichthyornis* is largely orthogonal to the palate, no different from earlier theropod dinosaurs (Fig. 4 *B* and *C*), making the protractor muscles best suited for postural roles, modulating excursions of the palate during feeding (18). Further, the long, rostral-projecting orbital process of the quadrate in *Ichthyornis* and *Hesperornis* would increase the moment arm for mPSTp about the jaw joint while simultaneously increasing the moment arm for protractor muscles about the otic joint (Fig. 4*D*), placing this muscle in ideal positions to modulate streptostylic motions of the quadrate. Moreover, the mandibular articulation of the quadrate in *Ichthyornis* and *Hesperornis* is plesiomorphic and bicondylar, as opposed to the tricondylar jaw joint observed in Neoaves [Fig. 4*D*; (23)]. The tricondylar jaw joint has been proposed to be a necessary "locking device" for coupled cranial kinesis (24), potentially limiting the types of kinetic excursions *Ichthyornis* and *Hesperornis* would have been capable of. The addition of a flexible frontonasal joint appears to be a turning point in early bird evolution wherein paleognath birds maintain largely stiff, arguably rhynchokinetic faces, while neognath birds become more kinetic via joint mobility (Fig. 3). These evolutionary trends likely represent alternate strategies to mitigate the potential for pathological cranial mobility in early birds, as demonstrated by *Ichthyornis*.

Innovations in the feeding apparatus remain drivers in major transformations in vertebrate evolution. Reorientations of jaw muscles and the cascade of mechanical adaptations frequently characterize the origins of major clades, as shown here in birds. The origins of cranial fenestration in tetrapods, the migration of muscle-attaching bones of the mandible into the middle ear of mammaliaforms (54), the shift from facial loading to palatal loading in lepidosaurs (55) and the further reorganization of the musculoskeletal system in kinetic snakes (56), and the reorientation and hypertrophy of jaw muscles in flat-headed crocodyliforms (57) all show how macroevolutionary biomechanics of feeding ecology and ultimately changes in cranial musculoskeletal mechanics are major drivers of vertebrate diversity.

Conclusions

The vertebrate skull is a composite organ with the unique challenges of facilitating feeding while protecting the brain and cranial sensory organs. Cranial design therefore reflects a tradeoff among these competing demands. Here, we show how dinosaurs and their living descendants, birds, mediated the spatial tradeoff between an expanding braincase and powerful jaw musculature. Shifting patterns of 3D jaw muscle vectors correspond with not only the inflation of the avian neurocranium but also a reorganization of palatal structures. These new jaw muscle arrangements influence intracranial mechanics in the avian skull by reorienting protractor muscles to better transmit forces through the pterygoid. Linkage mechanics illustrates that dinosaur skulls were likely immobile until Neognathae. Our approaches allow for the quantification of classic ideas in functional morphology with new nuance and provide the framework for rigorous investigations into the origins of cranial kinesis in birds.

Materials and Methods

3D models of dinosaur skulls were generated from a mix of CT-scanned and laser-scanned specimens which were variably segmented, cleaned, and smoothed in Avizo 9.1 (Thermofisher, Waltham, MA) and Geomagic Studio v7 (3D Systems, Rock Hill, SC) as well as previously published 3D models (*SI Appendix*, Table S1). 3D models of dinosaur skulls were used to model muscle forces. First, the models were imported to Geomagic Studio and aligned so that the origin is the mid-sagittal plan of the jaw joint axis and the *x* direction is mediolateral (positive being left), the *y* direction is dorsoventral (positive being dorsal), and *z* direction is rostrocaudal (positive being rostral). Muscle attachment sites were then isolated from the model and exported as stl files. The surface area and area centroid of the muscle attachment sites were computed in Avizo v9 (Thermo Fisher Scientific, Waltham, MA), and muscle attachment sites were determined via first-hand analysis of specimens and previous publications (e.g., refs. 8, 14, 16, and 58–60). See *SI Appendix*, Figs. S5–S11 for jaw muscle maps used in this study. Muscle abbreviations can be found in *SI Appendix*, Table S2.

Surface areas and centroid coordinates from jaw muscle attachment sites were then used to model jaw muscles as a frustum to create a muscle volume sensu Sellers et al. (61). This volume is defined by Eq. **1**:

$$V_{!} = \frac{m}{3} \cdot \left(A_{or} + A_{ins} + \left(\sqrt{A_{or} \cdot A_{ins}} \right) \right), \qquad [\mathbf{1}]$$

where $V_{!}$ is muscle volume, $l_{!}$ is centroid–centroid length of the muscle, $A_{*\#}$ is the area of the muscle origin site, and $A_{\$\%\&}$ is the area of the muscle insertion site. "Origin" and "insertion" were arbitrarily defined and do not have any effect on

the calculation of V_m. This volume can then be used to calculate physiological cross-sectional area (PCSA) with Eq. **2** (62):

$$\mathrm{PCSA} = \frac{V_m}{l_f} \cdot \cos(\theta), \quad [\mathbf{2}]$$

where l_f is muscle fiber length, and θ is the angle of pennation. PCSA can then be used to calculate muscle force using Eq. **3** (63):

$$F_m = \mathrm{PCSA} \cdot T_{specific}, \quad [\mathbf{3}]$$

where F_m is muscle force, and $T_{specific}$ is the specific tension of the muscle. We chose a value of 0.3 N/mm^2 for specific tension, following Hieronymus (64). Because F_m scales linearly with $T_{specific}$, the specific value is relatively unimportant and does not impact later steps in the analysis pathway. Muscle fiber length and pennation angle must be inferred in extinct taxa. For all taxa without reported values in the literature, fiber length was assumed to be two-thirds of the muscle length, and pennation angles for taxa without reported values are the same as those used for *T. rex* in Cost et al. (65). These muscle force data can then be used to create ternary diagrams of muscle vectors, be compared against braincase shape, and to analyze feeding mechanics.

Ternary diagrams display the orientation of jaw muscle force vectors (66). These diagrams were made in R using the package MuscleTernary (https://github.com/MiddletonLab/MuscleTernary). To better compare muscle force and orientation across a broad phylogenetic range of taxa, individual muscle forces were scaled to summed muscle force, creating a per-taxon, relative muscle force.

To test our hypotheses about the effect of braincase expansion on jaw muscle variation, we created a ratio describing braincase expansion by dividing the width of the braincase (greatest width of the temporal fossa of the neurocranium) by the width of the jaw joints (biquadrate width), as shown in Fig. 2*A*. To scale total jaw muscle to body size we performed a linear model regression of log-transformed total jaw muscle volume on log-transformed skull length (caudal edge of occiput to rostral tip of premaxilla). The residuals of this regression were then used to compare jaw muscle size against braincase expansion. We also performed this analysis on each individual muscle, as well as a grouping of the muscles found in the adductor chamber (*SI Appendix*, Figs. S3 and S4) to highlight differing effects of braincase expansion on different muscle volumes.

To understand the effects of novel jaw muscle arrangements on the feeding apparatus, we calculated muscle efficiency (57). Muscle efficiency is calculated with Eq. **4**:

$$E_m = \frac{F_{\#}}{F_m}, \quad [\mathbf{4}]$$

where E_m is muscle efficiency, $F_{\#}$ is the muscle force resultant, and F_m is the gross muscle force (57). This metric describes the estimated muscle force that is wasted by muscle force components canceling each other out (57). Ancestral state reconstruction of jaw muscle efficiency was performed using the R package ape (https://CRAN.R-project.org/package=ape) on a phylogeny of dinosaurs modified from Felice et al. (66). We consider muscles as being more efficient when they are vertically oriented in line with orthal feeding behaviors and muscle forces. This is largely the primitive condition of theropods (34). We consider jaw muscles less efficient relative to orthal orientations even though we acknowledge a rostrocaudally oriented muscle in a bird, for example, is still likely to be efficient for its behavioral needs.

To evaluate the presence of powered prokinesis, we calculated the amount of protractor muscle force that is axially transmitted along the pterygoid bone. This was accomplished by creating a vector describing the direction of the pterygoid using centroid coordinates at both the caudal and rostral ends of the pterygoid. The resultant protractor muscle force vector was then projected on to the pterygoid vector using Eq. **5**:

$$projF_{m/} = \frac{F_{mPPt} \cdot V_{pty}}{\left|V_{pty}\right|^2} \cdot V_{/3}, \quad [\mathbf{5}]$$

where $projF_{m/}$ is the projected protractor muscle force, $F_{m/}$ is the protractor muscle force, and $V_{/3}$ is the direction of the pterygoid. We then divided the projected protractor muscle force by the original protractor muscle force to create a percentage of protractor muscle force that is transmitted. Although there is no publicly available 3D model of *Ichthyornis* or *Hesperornis* to calculate the protractor muscle force vector and pterygoid vector from, estimation of these vectors was made possible via multiple, different 2D views (39, 41). Despite the lack of reliable pterygoid for *Ichthyornis,* the boundary conditions created by a present quadrate, palatine, and basicranium provide a basis for a reliable estimation of the orientation the pterygoid ought to be in. These data were plotted on a chimera model of *Ichthyornis* quadrate material from BHI 6421 and AMNH FARB 32773. Ancestral state reconstruction of protractor muscle force transmission was performed using the R package ape (https://CRAN.Rproject.org/package=ape) on a phylogeny of dinosaurs modified from Felice et al. (66). To quantify the kinetic capacity of a taxon's skull we employed linkage analysis (4). We quantified total linkage mobility with Eq. **6** (67):

$$M = \sum (f) - dn, \quad [\mathbf{6}]$$

where M is the total degrees of freedom of the linkage, f is the degrees of freedom for a given joint, d is the dimensionality constant (6 for 3D linkages), and n is the number of loops [four for non-avian dinosaur skulls as well as the primitive diapsid condition; (4, 53)]. The maximum degrees of freedom a joint may have is six (translations in three dimensions and rotations in three dimensions). Because solving for M only requires descriptions of joints and not fully articulated 3D models, we were able to expand our sample size for this analysis to capture extinct species that likely represent key steps in the evolution of cranial kinesis (e.g., refs. 7, 31–33, 44, and 68). We based our coding of individual joint degrees of freedom based off a search for key words in descriptions of joints. This creates a consistent character coding of individual joint morphologies that is meaningful even if the functional interpretations are erroneous. Ancestral state reconstruction of linkage mobility was performed using the R package ape (https://CRAN.R-project.org/package=ape) on a phylogeny of dinosaurs modified from Felice et al. (66).

Data, Materials, and Software Availability. Models are available via download on Sketchfab and Open Science Framework (OSF). Data from dinosaur material are available in part through Sketchfab and OSF, or the authors by request. Data type–3D models (.stl files) data have been deposited in Sketchfab and OSF (https://osf.io/2kpdb/) (38). Previously published data were used for this work (59, 69).

ACKNOWLEDGMENTS. We thank Armita Manafzadeh, John Fortner, Marc Jones, Callum Ross, Zhe-Xi Luo, Peishu Li, Rachel Rozin, Emily Hillan, Kara Feilich, and Hannah Farrell for insightful discussion, assistance, and feedback on this project. We thank Megan Sims and KU Biodiversity Institute and Natural History Museum Vertebrate Paleontology Collections for access to *Hesperornis*and *Ichthyornis* specimens. We thank Peter Larson at the Black Hills Institute and Art Anderson at Virtual Surface for permission to use the 3D model of BHI 3033. We thank Dan Field and Juan Benito for models of BHI 6421 and AMNH FARB 32773. This study was funded by MU LS UROP, NSF IOS 1457319, NSF EAR 1631684, NSF IOS 520100, and NIH NINDS T32NS121763.

Author affiliations: [a]Department of Organismal Biology and Anatomy, University of Chicago, Chicago, IL 60637; [b]Department of Biology, Albright College, Reading, PA 19612; [c]Department of Engineering, University of Southern Indiana, Evansville, IN 47712; [d]Division of Biological Sciences, University of Missouri, Columbia, MO 65211; [e]Department of Biomedical Sciences, Heritage College of Osteopathic Medicine, Ohio Center for Ecology and Evolutionary Studies, Ohio University, Athens, OH 45701; and [f]Department of Pathology and Anatomical Sciences, University of Missouri, Columbia, MO 65212

1. R. G. Bout, G. A. Zweers, The role of cranial kinesis in birds. *Comp. Biochem. Physiol. A, Mol. Integr. Physiol.* **131**, 1197–1205 (2001), 10.1016/s1095-6433(01)00470-6.
2. H. Hu *et al.*, Evolution of the vomer and its implications for cranial kinesis in Paraves. *Proc. Natl. Acad. Sci. U.S.A.* **116**, 19571–19578 (2019), 10.1073/pnas.1907754116.
3. J. Benito *et al.*, Cretaceous ornithurine supports a neognatheous crown bird ancestor. *Nature* **612**, 100–105 (2022), 10.1038/s41586-022-05445-y.
4. A. M. Olsen, M. W. Westneat, Linkage mechanisms in the vertebrate skull: Structure and function of three-dimensional, parallel transmission systems. *J. Morphol.* **277**, 1570–1583 (2016), 10.1002/jmor.20596.
5. A. M. Balanoff *et al.*, Evolutionary origins of the avian brain. *Nature* **501**, 93–96 (2013), 10.1038/nature12424.
6. M. Fabbri *et al.*, The skull roof tracks the brain during the evolution and development of reptiles and birds. *Nat. Ecol. Evol.* **1**, 1543–1550 (2017), 10.1038/s41559-017-0288-2.

7. C. R. Torres, M. A. Norell, J. A. Clarke, Bird neurocranial and body mass evolution across the end-Cretaceous mass extinction: The avian brain shape left other dinosaurs behind. *Sci. Adv.* **7**, eabg7099 (2021), 10.1126/sciadv.abg7099.
8. C. M. Holliday, L. M. Witmer, Cranial kinesis in dinosaurs: Intracranial joints, protractor muscles, and their significance for cranial evolution and function in diapsids. *J. Vertebr. Paleontol.* **28**, 1073–1088 (2008), 10.1671/0272-4634-28.4.1073.
9. L. Dollo, Cinquième note sur les dinosauriens de Bernissart. *Bull. Mus. R. Hist. Nat. Belg.* **3**, 129–146 (1884).
10. J. Verslyus, Streptostylie bei dinosauriern, nebst bemerkungen über die verwandtschaft der vögel und dinosaurier. *Zool. Jarb. Anat.* **30**, 175–260 (1910).
11. H. F. Osborn, Crania of Tyrannosaurus and Allosaurus. *Mem. Am. Mus. Nat. Hist.* **1**, 1–32 (1912), 10.5281/zenodo.2784073.
12. E. J. Rayfield *et al.*, Cranial design and function in a large theropod dinosaur. *Nature* **409**, 1033–1037 (2001), 10.1038/35059070.
13. I. N. Cost *et al.*, Palatal biomechanics and its significance for cranial kinesis in *Tyrannosaurus rex*. *Anat. Rec.* **303**, 999–1017 (2019), 10.1002/ar.24219.
14. A. T. Wilken *et al.*, Connecting the chondrocranium: Biomechanics of the suspensorium in reptiles. *Vertebr. Zool.* **70**, 275–290 (2020), 10.26049/VZ70-3-2020-02.
15. M. Mezzasalma, N. Maio, F. M. Guarino, To move or not to move: Cranial joints in European gekkotans and lacertids, an osteological and histological perspective. *Anat. Rec.* **297**, 463–472 (2014), 10.1002/ar.22827.
16. R. G. Bout, H. P. Zeigler, Jaw muscle (EMG) activity and amplitude scaling of jaw movements during eating in pigeon (*Columba livia*). *J. Comp. Physiol. A* **174**, 433–442 (1994), 10.1007/BF00191709.
17. S. W. S. Gussekloo, R. G. Bout, Cranial kinesis in palaeognathous birds. *J. Exp. Biol.* **208**, 3409–3419 (2005), 10.1242/jeb.01768.
18. A. T. Wilken *et al.*, The roles of joint tissues and jaw muscles in the palatal biomechanics of the savannah monitor (*Varanus exanthematicus*) and their significance for cranial kinesis. *J. Exp. Biol.* **222**, jeb201459 (2019), 10.1242/jeb.201459.
19. P. J. Currie, New information on the anatomy and relationships of *Dromaeosaurus albertensis* (Dinosauria: Theropoda). *J. Vertebr. Paleontol.* **15**, 576–591 (1995), 10.1080/02724634.1995.10011250.
20. K. K. Smith, Mechanical significance of streptostyly in lizards. *Nature* **283**, 778–779 (1980), 10.1038/283778a0.
21. M. M. Dawson *et al.*, Kinematics of the quadrate bone during feeding in mallard ducks. *J. Exp. Biol.* **214**, 2036–2046 (2011), 10.1242/jeb.047159.
22. S. L. Payne, C. M. Holliday, M. K. Vickaryous, An osteological and histological investigation of cranial joints in geckos. *Anat. Rec.* **294**, 399–405 (2011), 10.1002/ar.21329.
23. A. M. Bailleul, L. M. Witmer, C. M. Holliday, Cranial joint histology in the mallard duck (*Anas platyrhynchos*): New insights on avian cranial kinesis. *J. Anat.* **230**, 444–460 (2017), 10.1111/joa.12562.
24. W. J. Bock, Kinetics of the avian skull. *J. Morphol.* **114**, 1–52 (1964), 10.1002/jmor.1051140102.
25. P. Bühler, "Functional anatomy of the avian jaw apparatus" in *Form and Function in Birds*, A. S. King, B. K. McClelland, Eds. (Academic Press, London, UK, 1981), **vol. 2**.
26. E. J. Rayfield, Using finite-element analysis to investigate suture morphology: A case study using large carnivorous dinosaurs. *Anat. Rec.* **283A**, 349–365 (2005), 10.1002/ar.a.20168.
27. A. Elzanowski, G. Mayr, Multiple origins of secondary temporal fenestrae and orbitozygomatic junctions in birds. *J. Zool. Syst. Evol. Res.* **56**, 248–269 (2017), 10.1111/jzs.12196.
28. A. Elzanowski, D. S. Peters, G. Mayr, Cranial morphology of the Early Cretaceous bird Confuciusornis. *J. Vertebr. Paleontol.* **38**, e1439832 (2018), 10.1080/02724634.2018.1439832.
29. M. Wang, H. Hu, A comparative morphological study of the jugal and quadratojugal in early birds and their dinosaurian relatives. *Anat. Rec.* **300**, 62–75 (2017), 10.1002/ar.23446.
30. M. Wang *et al.*, Cretaceous bird with dinosaur skull sheds light on avian cranial evolution. *Nat. Commun.* **12**, 3890 (2021), 10.1038/s41467-021-24147-z.
31. M. Wang *et al.*, Insight into the evolutionary assemblage of cranial kinesis from a Cretaceous bird. *eLife* **11**, e81337 (2022), 10.7554/eLife.81337.
32. H. Hu *et al.*, Cranial osteology and paleobiology of the Early Cretaceous bird *Jeholornis prima* (Aves: Jeholornithiformes). *Zool. J. Linn. Soc.* **198**, 1–20 (2022), 10.1093/zoolinnean/zlac089.
33. Z. Li *et al.*, Decoupling the skull and skeleton in a Cretaceous bird with unique appendicular morphologies. *Nat. Ecol. Evol.* **7**, 20–31 (2023), 10.1038/s41559-022-01921-w.
34. C. M. Holliday, New insights into dinosaur jaw muscle anatomy. *Anat. Rec.* **292**, 1246–1265 (2009), 10.1002/ar.20982.
35. B. S. Bhullar *et al.*, How to make a bird skull: Major transitions in the evolution of the avian cranium, paedomorphosis, and the beak as a surrogate hand. *Integr. Comp. Biol.* **56**, 389–403 (2016), 10.1093/icb/icw069.
36. D. T. Ksepka *et al.*, Tempo and pattern of avian brain size evolution. *Curr. Biol.* **30**, 2026–2036 (2020), 10.1016/j.cub.2020.03.060.
37. D. J. Field *et al.*, Late Cretaceous neornithine from Europe illuminates the origin of crown birds. *Nature* **579**, 397–401 (2020), 10.1038/s41586-020-2096-0.
38. A. T. Wilken *et al.*, From "Avian cranial kinesis is the result of increased encephalization during the origin of birds." Open Science Framework. https://osf.io/2kpdb/. Deposited 19 February 2025.
39. D. J. Field *et al.*, Complete Ichthyornis skull illuminates mosaic assembly of the avian head. *Nature* **557**, 96–100 (2018), 10.1038/s41586-018-0053-y.
40. G. J. Dyke *et al.*, Europe's last Mesozoic bird. *Naturwissenschaften* **89**, 408–411 (2002), 10.1007/s00114-002-0352-9.
41. P. D. Gingerich, Evolutionary significance of the Mesozoic toothed birds. *Smithson. Contrib. Paleobiol.* **27**, 23–33 (1976).
42. A. Bell, L. M. Chiappe, Anatomy of Parahesperornis: Evolutionary mosaicism in the Cretaceous Hesperornithiformes (Aves). *Life* **10**, 62 (2020), 10.3390/Life10050062.
43. P. Bühler, L. D. Martin, L. M. Witmer, Cranial kinesis in the Late Cretaceous birds Hesperornis and Parahesperornis. *Auk* **105**, 111–122 (1988), 10.1093/auk/105.1.111.
44. R. L. Zusi, A functional and evolutionary analysis of rhynchokinesis in birds. *Smithson. Contrib. Zool.* **395**, 1–40 (1984).
45. G. A. Zweers, H. Berkhoudt, J. C. Vanden Berge, Behavioral mechanisms of avian feeding. *Adv. Comp. Physiol. Biol.* **18**, 243–279 (1994), 10.1007/978-3-642-57906-6_9.
46. J. Soons *et al.*, Multi-layered bird beaks: A finite-element approach towards the role of keratin in stress dissipation. *J. R. Soc. Interface* **9**, 1787–1797 (2012), 10.1098/rsif.2011.0910.
47. A. W. Crompton, The development of the chondrocranium of *Spheniscus demersus* with special reference to the columella auris of birds. *Acta Zool.* **34**, 71–146 (1953).
48. L. M. Chiappe, M. A. Norell, J. A. Clark, The skull of a relative of the stem-group bird Mononykus. *Nature* **392**, 275–278 (1998), 10.1038/32642.
49. G. De Beer, The development of the vertebrate skull. *Nature* **142**, 4–5 (1938).
50. M. M. Zaher, A. M. Abu-Taira, A review on the avian viscerocranium. *J. Basic Appl. Zool.* **75**, 46–53 (2016), 10.1016/j.jobaz.2016.07.001.
51. K. C. Woronowicz, R. A. Schneider, Molecular and cellular mechanisms underlying the evolution of form and function in the amniote jaw. *EvoDevo* **10**, 17 (2019), 10.1186/s13227-019-0131-8.
52. J. Klembara, Ontogeny of the palatoquadrate and adjacent lateral cranial wall of the endocranium in prehatching *Alligator mississippiensis* (Archosauria: Crocodylia). *J. Morphol.* **262**, 644–658 (2004), 10.1002/jmor.10266.
53. A. M. Olsen, A mobility-based classification of closed kinematic chains in biomechanics and implications for motor control. *J. Exp. Biol.* **222**, jeb195735 (2019), 10.1242/jeb195735.
54. A. Crompton, W. Hylander, "Changes in masticatory function following the acquisition of a dentary-squamosal jaw articulation" in *The Ecology and Biology of Mammal-Like Reptiles*, N. Hotton, P. D. Maclean, J. J. Roth, E. C. Roth, Eds. (Smithsonian Institution Press, Washington, DC, 1986), pp. 263–282.
55. M. Moazen *et al.*, Biomechanical assessment of evolutionary changes in the lepidosaurian skull. *Proc. Natl. Acad. Sci. U.S.A.* **106**, 8273–8277 (2009), 10.1073/pnas.0813156106.
56. D. Cundall, Activity of head muscles during feeding by snakes: A comparative study. *Am. Zool.* **23**, 383–396 (1983).
57. K. C. Sellers *et al.*, The effects of skull flattening on suchian jaw muscle evolution. *Anat. Rec.* **305**, 2791–2822 (2022), 10.1002/ar.24912.
58. A. Elzanowski, Cranial and eyelid muscles and ligaments of the tinamous (Aves: Tinaformes). *Zool. Jahrb. Anat. Ontog. Tiere* **116**, 63–118 (1987).
59. S. Lautenschlager *et al.*, Cranial anatomy of *Erlikosaurus andrewsi* (Dinosauria, Therizonosauria): New insights based on digital reconstruction. *J. Vertebr. Paleontol.* **34**, 1937–2809 (2014), 10.1080/02724634.2014.874529.
60. M. E. H. Jones *et al.*, Digital dissection of the head of rock dove (*Columba livia*) using contrast-enhanced computed tomography. *Zool. Lett.* **5**, 17 (2019), 10.1186/s40851-019-0129-z.
61. K. C. Sellers *et al.*, Ontogeny of bite force in a validated biomechanical model of the American alligator. *J. Exp. Biol.* **220**, 2036–2046 (2017), 10.1242/jeb156281.
62. R. D. Sacks, R. R. Roy, Architecture of the hind limb muscles of cats: Functional significance. *J. Morphol.* **173**, 185–195 (1982), 10.1002/jmor.1051730206.
63. C. Gans, Fiber architecture and muscle function. *Exerc. Sport Sci. Rev.* **10**, 160–207 (1982).
64. T. L. Hieronymus, Quantitative microanatomy of jaw muscle attachment in extant diapsids. *J. Morphol.* **267**, 954–967 (2006), 10.1002/jmor.10450.
65. I. N. Cost *et al.*, 2D and 3D visualizations of archosaur jaw muscle mechanics, ontogeny and phylogeny using ternary diagrams and 3D modeling. *J. Exp. Biol.* **225**, jeb243216 (2019), 10.1242/jeb243216.
66. R. N. Felice *et al.*, Decelerated dinosaur skull evolution with the origin of birds. *PLoS Biol.* **18**, e3000801 (2020), 10.1371/journal.pbio.3000801.
67. A. Müller, Generic mobility of rigid mechanisms. *Mech. Mach. Theory* **44**, 1240–1255 (2009), 10.1016/jmechmachtheory.2008.08.002.
68. A. Elzanowski, A novel reconstruction of the skull of Archaeopteryx. *Neth. J. Zool.* **51**, 207–215 (2001), 10.1163/156854201X00279.
69. S. Lautenschlager, Estimating cranial musculoskeletal constraints in theropod dinosaurs. *R. Soc. Open Sci.* **2**, 150495 (2015).